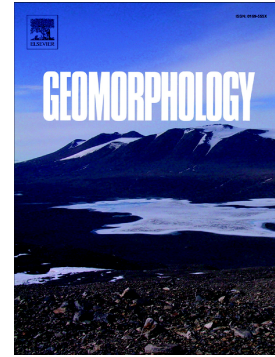


## Journal Pre-proof

Decadal shoreline erosion and recovery of beaches in modified and natural estuaries

Thomas E. Fellowes, Ana Vila-Concejo, Shari L. Gallop, Ryan Schosberg, Vincent de Staercke, John L. Largier



PII: S0169-555X(21)00292-0

DOI: <https://doi.org/10.1016/j.geomorph.2021.107884>

Reference: GEOMOR 107884

To appear in: *Geomorphology*

Received date: 5 February 2021

Revised date: 13 July 2021

Accepted date: 27 July 2021

Please cite this article as: T.E. Fellowes, A. Vila-Concejo, S.L. Gallop, et al., Decadal shoreline erosion and recovery of beaches in modified and natural estuaries, *Geomorphology* (2021), <https://doi.org/10.1016/j.geomorph.2021.107884>

This is a PDF file of an article that has undergone enhancements after acceptance, such as the addition of a cover page and metadata, and formatting for readability, but it is not yet the definitive version of record. This version will undergo additional copyediting, typesetting and review before it is published in its final form, but we are providing this version to give early visibility of the article. Please note that, during the production process, errors may be discovered which could affect the content, and all legal disclaimers that apply to the journal pertain.

© 2021 Elsevier B.V. All rights reserved.

# Decadal shoreline erosion and recovery of beaches in modified and natural estuaries

Thomas E. Fellowes<sup>1,2\*</sup>, Ana Vila-Concejo<sup>1,2</sup>, Shari L. Gallop<sup>3,4</sup>, Ryan Schosberg<sup>1,2</sup>,  
Vincent de Staercke<sup>5,6</sup>, John L. Largier<sup>7,8</sup>

<sup>1</sup>Geocoastal Research Group, School of Geosciences, Faculty of Science, University of Sydney, Sydney, Australia.

<sup>2</sup>Marine Studies Institute, Faculty of Science, University of Sydney, Sydney, Australia

<sup>3</sup>School of Science, University of Waikato, Tauranga, New Zealand

<sup>4</sup>Environmental Research Institute, University of Waikato, Hamilton, New Zealand

<sup>5</sup>Geographic Information Systems Laboratory, École Polytechnique Fédérale de Lausanne, Switzerland

<sup>6</sup>Department of Earth and Environmental Sciences, Macquarie University, Sydney, Australia

<sup>7</sup>Coastal and Marine Sciences Institute, University of California Davis, Bodega Bay, United States of America

<sup>8</sup>Department of Environmental Science and Policy, University of California Davis, Davis, United States of America

## **\*Corresponding Author:**

Thomas E. Fellowes

Tel: +61 403 921 579

Email: [thomas.fellowes@sydney.edu.au](mailto:thomas.fellowes@sydney.edu.au)

Postal Address: Geocoastal Research Group, Madsen Building (F09), The University of Sydney, New South Wales, 2006, Australia.

**ABSTRACT**

Sandy beaches in estuaries and bays (BEBs) are common landforms on the coasts of many major cities. They exist under a wide range of settings and their morphology is controlled by their distance from the estuary/bay entrance, exposure to different types of waves (e.g., ocean swells vs locally generated wind waves), proximity to flood-tide delta/shoals, and anthropogenic interventions (e.g., dredging, groynes). Both swell waves propagating into estuaries/bays and locally generated wind waves can erode BEBs. However, more understanding of BEB storm erosion and recovery over decadal timescales is needed, as they typically respond slower than open coast beaches. Here we present decadal shoreline behaviours of nine BEBs from two estuarine systems in SE Australia are presented in this study, using 76 years of aerial imagery (1941–2017). We quantify and compare decadal behaviour between beaches, developing a new typology of BEBs based on shoreline evolution. We identify four decadal behaviours: *prograding*, *quasi-stable*, *retreating* and *storm relict* – and assess the influence of flood-tide deltas, river mouths, distance from the ocean entrance, and anthropogenic interventions. Swell-exposed BEBs near the entrance are *quasi-stable* and recover after storms at rates comparable with open coast beaches (<3 years). In contrast, BEBs further from the entrance and those with less swell exposure, have slower recovery timescales (3–15 years) and will only be *quasi-stable* if storms are sufficiently infrequent. Thus, long-term behaviour is controlled by storm return timescales. *Prograding* BEBs are typically far from the entrance, where fluvial and tidal processes dominate and erosion events due to wind waves are less pronounced. Whether BEBs recover (*quasi-stable*), partially recover between storms (*retreating*) or never recover (*storm relict*) relates to storm frequency, recovery rates and proximity to sediment sources and sinks (e.g., dredge

sites, flood-tide deltas, tidal channels) and anthropogenic interventions. Findings will help to better understand and manage BEB shorelines in major cities.

## KEYWORDS

Sheltered beach; low energy beach; storm erosion; beach

## 1. INTRODUCTION

Sandy beaches in estuaries and bays (BEBs) are common landforms worldwide, found in many major coastal cities. Their morphology depends on multiple factors, including sediment supply, geological setting, proximity to flood-tide deltas, swell and local wind wave exposure (Vila-Concejo et al., 2020). In some cases, anthropogenic interventions such as dredging, groynes or revetments also influence BEBs (Lowe and Kennedy, 2016). BEBs are typically considered steep and narrow, and have been traditionally classified as 'low-energy' and dominated by local wind-waves and alongshore sediment transport (Nordstrom and Jackson, 2012). However, ocean swell and infra-gravity waves that propagate into estuaries, as well as tides, currents and boat wakes may also be important for BEB morphodynamics (Jackson, 1995). Although BEBs are semi-protected from ocean waves, they can still experience erosion events due to storm waves from certain directions that can enter the estuary/bay (Vila-Concejo et al., 2010). When this happens, BEBs can experience significant erosion, proportionate or greater than open coast beaches, with slow or limited post-storm recovery (Gallop et al., 2020).

There is a lack of understanding of the mechanisms that control BEB recovery for both the subaerial and intertidal sediments (Nordstrom and Jackson, 2012), and it is clear that BEBs cannot be considered as scaled-down versions of open coast beaches (Vila-Concejo et al., 2020). While it is thought that there may be insufficient

wave energy to facilitate full recovery after storm erosion, BEBs would not exist without sufficient wave energy to build them (Nordstrom and Jackson, 2012). Rather, it appears that beaches typically protected from swell recover at slower rates than open coast beaches (Costas et al., 2005). Previous BEB studies have focused largely on timescales of months to a few years (Gallop et al., 2020; Harris et al., 2020; Vila-Concejo et al., 2010) and it is not known if BEBs can recover fully over longer timescales – or if erosion is a one-way process for some BEB settings, leading to progressive shoreline retreat (Harris et al., 2020). For example, sediments eroded from BEBs can be transported to nearshore sediment sinks, such as flood-tide deltas/shoals (Austin et al., 2018; Vila-Concejo et al., 2011; Vila-Concejo et al., 2007). In some cases, these sediments can be returned to the beach (Austin et al., 2018; Jackson, 1995), but are sometimes permanently lost to the beach system. Beach sediment may be imported through alternate pathways like alongshore transport or offshore sources under certain conditions (Vila-Concejo et al., 2010).

BEBs can exhibit distinct behaviours and morphology following storms (Carrasco et al., 2012; Costas et al., 2005). For example, Eulie et al. (2017) show how backbarrier shorelines in the Albemarle-Pamlico estuary system in North Carolina (USA) have been retreating episodically due to storms since the 1950s, at a mean rate of 0.5 m/year. Further, Qiao et al. (2018) describe how 50 years of reclamation of low-lying estuarine shorelines in Shanghai (China) causes unwanted erosion of adjacent BEBs and low-lying coastal areas, and Gallop et al (2020) show both partial and full recovery of BEBs in New South Wales (Australia) following storm erosion. These studies highlight the tendency for slow or incomplete recovery of BEBs in contrast to open coast beaches. It appears that a fine balance exists between the frequency and severity of erosion and the rate of accretion leading to recovery. Moreover, there

have been few studies of the influence of anthropogenic interventions such as dredging, reclamation, seawalls and groynes. These can alter wave climate and shorefaces (Nordstrom, 1992), beach planform, subaerial morphology and shoreline positions (Lowe and Kennedy, 2016), and sediment source/sink pathways (Austin et al., 2018). For example, Carrasco et al. (2012) report decadal change to BEB shorelines in a barrier estuary in the Algarve (Portugal), which eroded up to 0.22 m/year due to the dredging of an adjacent navigation channel. Thus, changes to estuary/bay shorelines (natural or anthropogenic) can pose different complex coastal management and planning challenges.

To understand the long-term cycle of storm erosion and between-storm recovery for beaches in modified and natural estuaries and bays, the shoreline position (i.e., subaerial beach width) was quantified and tracked for nine BEBs over several decades. This study has three objectives: (1) to develop a behavioural typology of decadal BEB shoreline evolution; (2) to determine the influence of proximal geomorphological features such as flood-tide deltas or river mouths, and the distance of BEB from ocean entrance; and (3) to assess the role of anthropogenic interventions on decadal BEB shoreline behaviour. This understanding of the evolution of BEBs over decadal scales is critical for effective coastal management and planning.

## **2. STUDY AREA**

### **2.1. Sites**

The focus of this study is on two estuaries in the Sydney metropolitan area in New South Wales, Australia (Fig. 1a). Both contain a broad range of BEBs (Fig. 1b-g; Table 1) with a variety of distances from estuary entrance, locations relative to flood-

tide delta or river mouth, beach orientations, exposure to swell or wind waves, geological settings and anthropogenic interventions such as reclamation or groynes (Gallop et al., 2020). In this study Aboriginal place names are used where possible to acknowledge the pre-colonial and continuing histories in the region.

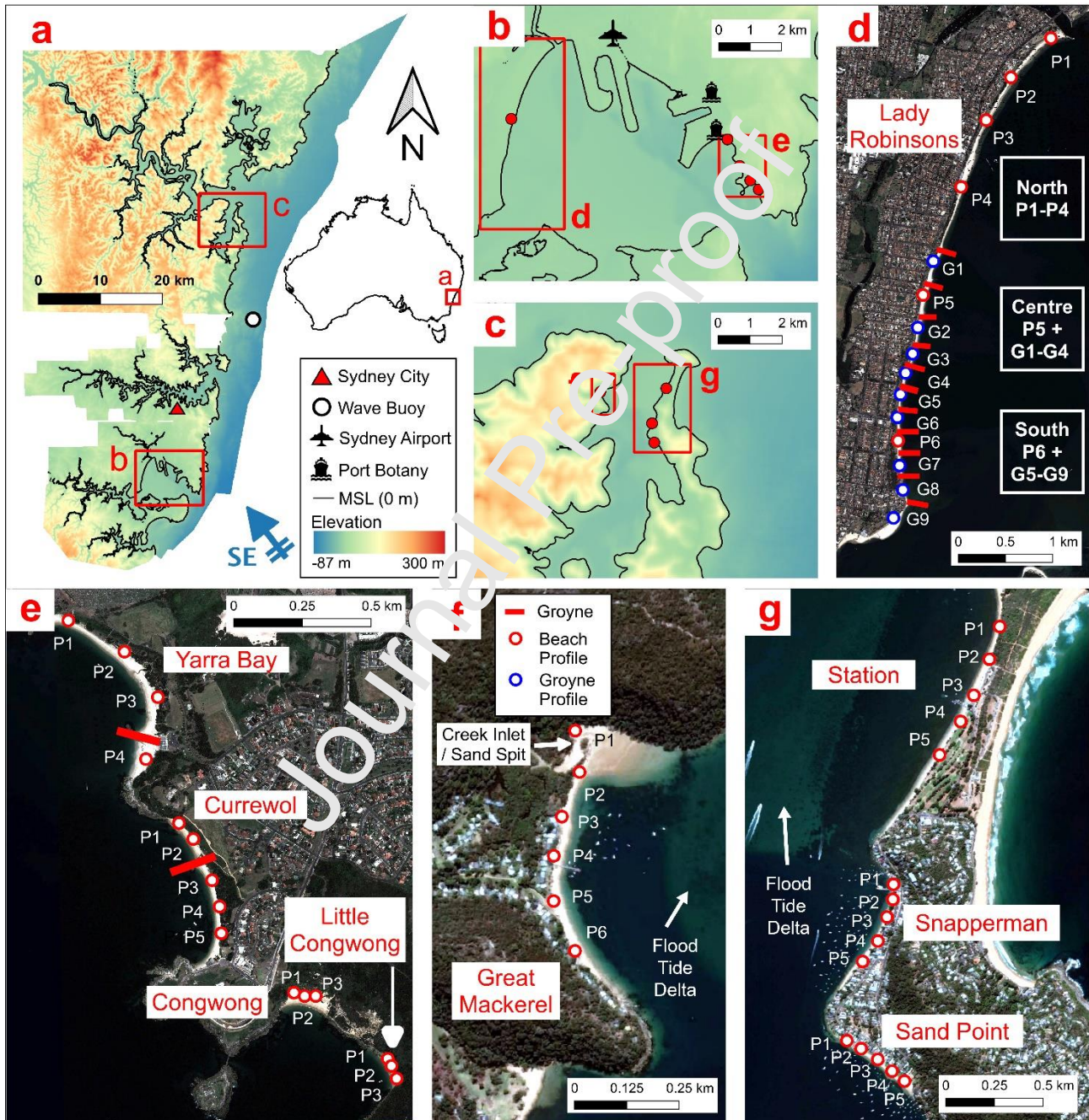


**Figure 1.** Study areas in (a) Australian and Sydney context showing (b) Kamay (Botany Bay) and (c) Garigal (Pittwater) with the Sydney offshore Waverider buoy

(black/white circle). Kamay BEBs are (d) Lady Robinsons, (e) Yarra Bay, Currewol (Frenchmans), Congwong and Little Congwong. Garigal BEBs are (f) Great Mackerel, (g) Station, Snapperman and Sand Point. BEBs have beach profiles (red/white circles), groyne profiles (blue/white circles) and groyne locations (red lines). Digital elevation models (a–c) are combined from Wilson and Power (2018a); Wilson and Power (2018b); Wilson and Power (2018c) and satellite images from Google Earth.

### 2.1.1. Garigal

Pittwater estuary, henceforth referred to by its Aboriginal name Garigal, is a tide-dominated, drowned river valley 28 km north of Sydney (Roy et al., 2001), that forms part of the Broken-Bay-Hawkesbury-River estuary (Fig. 1a, c). Garigal's entrance orientation is N–NE, and thus receives waves that propagate through the estuary entrance unmodified from the NE and refracted from the E-SE (Short, 1993). The estuary is 10 km long and 1 km wide and has an area of  $\sim 18.4 \text{ km}^2$  (OEH, 2018). The mean estuary depth is 9.9 m and the maximum depth is 22 m (OEH, 2018). The sediments are primarily sandy, with a flood-tide delta that extends  $\sim 2.5 \text{ km}$  into the estuary. Seagrass meadows in the estuary have declined since the 1940s (Cowell and Nelson, 1991). The net southward littoral drift within estuary through tidal channels along the western exposed shore and across the flood-tide delta of the Broken-Bay-Hawkesbury-River estuary is estimated at  $1500 (\pm 300) \text{ m}^3/\text{year}$  between 1940–1990 (Kulmar and Gordon, 1987).

**Table 1:** The BEBs are described in Short (1993), and their length, orientation, distance from the entrance to the open ocean and beach/groyne profiles locations as measured in this study.

	BEB	Orientation	Beach Length (m)	Distance from Entrance (km)	Beach/Groyne Profiles
Garigal	Great Mackerel	E	640	1.9	5 (P2–P6)
	Station	NW	1500	1.2	5 (P1–P5)
	Snapperman	NW	640	2.2	5 (P1–P5)

Kamay	Sand Point	SW	470	2.7	5 (P1–P5)
	Yarra Bay	SW	680	2.6	4 (P1–P4)
	Currewol	W	550	1.8	5 (P1–P5)
	Congwong	SE	160	1.3	3 (P1–P3)
	Little Congwong	SW	130	1.2	3 (P1–P3)
	Lady Robinsons	E	5500	8.2	15 (P1–P6; G1–G9)

This study includes 4 BEBs in the Garigal estuary (Fig. 1c, f–g; Table 1). The embayed Great Mackerel Beach on the western shore of Garigal is swash-aligned, adjacent to the flood-tide delta, and exposed to NE swell waves (Fig. 1f). It has a creek inlet (behind P2) that was artificially moved 100 m towards the northern headland in the late 1980s to protect beachfront properties from shoreline retreat (Cowell and Nelson, 1991). On the eastern shore of Garigal the focus is on three drift-aligned beaches. Station Beach is on the backshore of a sand barrier (shared with the open coast Palm Beach) (Fig. 1g). Further south is Snapperman Beach, which lies north of a low-lying promontory and adjacent to the flood-tide delta and a nearshore tidal channel; the centre and southern portions of this beach are backed by a seawall and residential properties (Fig. 1g). Sand Point BEB occupies the south side of the same promontory, with a seawall along the northern portion of the beach, which is also backed by residential properties (Short, 1993).

### 2.1.2. Kamay

Botany Bay, henceforth referred to by its Aboriginal name Kamay, is a marine-dominated open embayment 12 km south of Sydney (Roy et al., 2001) (Fig. 1a–b). Kamay occupies ~39.6 km<sup>2</sup> and has a maximum width and length of 5 km and 8 km. The average depth is 11.4 m and the bay has a SE-facing entrance that is 1.1 km wide (OEH, 2018). Two rivers enter Kamay: The Cooks River in the NW of the estuary and the Tucoerah (Aboriginal name for Georges River) in the SW (Fig. 1b). The estuary is composed primarily of sandy sediments with some mud around the

extensive mangrove habitats on the southern shore (Jones, 1981). The estuary has been heavily modified since 1900 (Fig. 2), with interventions including river realignment, dredging and reclamation to build and extend the port and airport, and the construction of groynes, rock armaments and a revetment (Fig. 1b). Meanwhile ongoing maintenance has included dredging the bay floor and shipping channels to nourish eroding beaches.

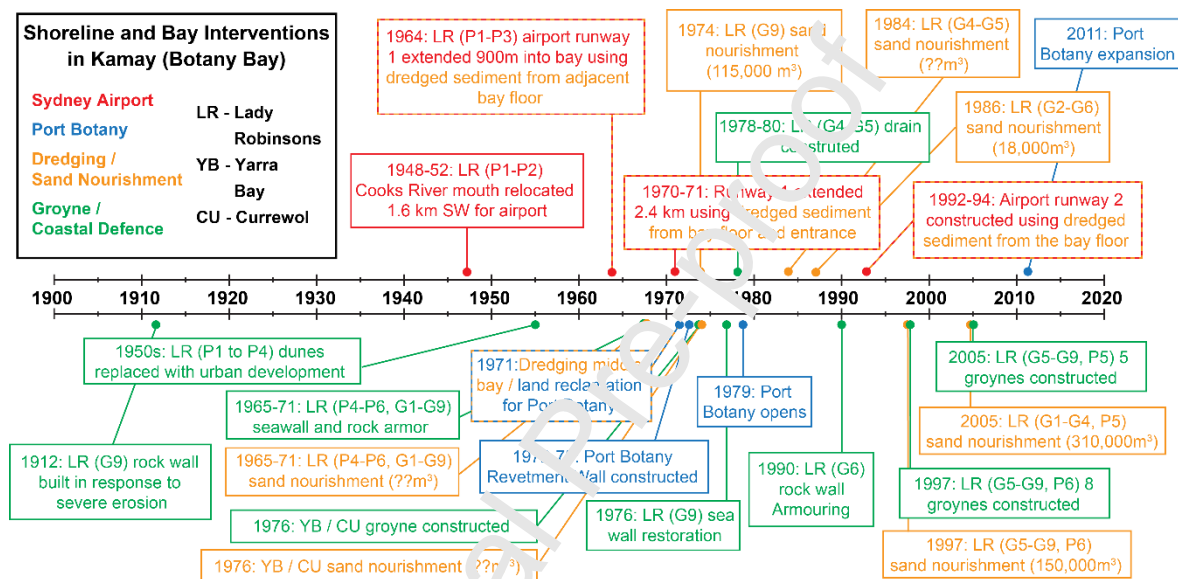


**Figure 2:** Timeline of anthropogenic interventions to bay shorelines and BEBs in Kamay since 1900. BEB and profile locations are coloured by intervention type (red/blue/yellow/green or multiple). Collated from Aijaz and Treloar (2003); Bryant and Kidd (1975); Cowen and Kannane (2000); Davies and McIlquham (2011); Frost (2011); Jones (1981).

This study includes 5 BEBs in Kamay, including Congwong and Little Congwong (Aboriginal names for beaches in La Perouse), Currewol (Aboriginal name for Frenchmans Bay) and Yarra Bay (Aboriginal name for Phillip Bay) on the NE shore near the entrance and Lady Robynsons on the western shore (Fig. 1d–e; Table 1). Congwong and Little Congwong are swash-aligned pocket beaches inside a larger embayment. They are both backed by well-developed dunes and being the closest to

the entrance, are exposed to S–SE swell waves (Short, 1993). Currewol and Yarra Bay, also swash aligned, have low-lying vegetated dunes and Yarra is adjacent to the Port Botany Revetment Wall (Fig. 1b, e). These two BEBs are west-facing and each have a central groyne built in 1976 (Cowell and Kannane, 2000). Lady Robinsons, which is drift-aligned, is bound by the Cooks and Tucoerah Rivers (Fig. 1d). This beach is at the front of a prograding barrier that is heavily modified and adjacent to the airport in the north. Groynes were constructed along the central and southern beach in 1997 and 2005 (Cowell and Kannane, 2000) (Fig. 1d; Fig. 2).

## 2.2. Climate

### 2.2.1. General wind, wave and tide conditions

The Sydney region in SE Australia has NE prevailing winds with mean speed at 09h00 of 10.6 km/h. The region is microtidal with a mean spring tidal range of 1.25 m (Harley et al., 2017). The wave climate is swell dominated with moderate to high wave energy that typically originates from the S-SE ( $\theta = 135^\circ$ ) and is characterised by mean offshore significant wave heights ( $H_s$ ) of 1.6 m, mean periods ( $T_z$ ) of 6 s and peak periods of 10 s ( $T_p$ ) (Shand et al., 2010). Individual storms are defined as events with  $H_s > 3$  m (95<sup>th</sup> percentile  $H_s$ ) for at least 6 hours, separated by at least 24 hours of gentle wave conditions (Shand et al., 2010). Storm clusters are groups of storms separated by less than a month, following Birkemeier et al. (1999). Storms occur year-round but are typically more common during Austral autumn and winter (April to August). Storms make landfall from a range of directions (NE to S) and are produced by mid-latitude cyclonic, low-pressure systems, extratropical low-pressure systems (East Coast Lows, ECLs) and lows to the east of Australia (Short and Trenaman, 1992). ECLs are a main source of extreme beach erosion and damage to

coastal infrastructure on this coast (Harley et al., 2016). Storm frequency is controlled by Pacific Ocean climate patterns, including El Niño Southern Oscillation, Southern Annular Mode and Pacific Decadal Oscillation (Shand et al., 2010). Storm surges are typically small (< 0.7 m) due to the region's narrow continental shelf (Harley et al., 2017).

### 2.2.2. Major storms

The Sydney region has experienced 21 major storms (wave events) between 1941 and 2017. Of these storms (full details and sources in Supplementary Table S1), those that eroded shorelines include:

- Cluster of two storms in June 1950 from NE–SE with remarkable rainfall, widespread flooding and substantial coastal erosion (Australian Bureau of Meteorology, 2015).
- Cluster of three storms in May–June 1974 from E–NE/E–SE, considered the most erosive event in the region since measured records began and damaging coastal infrastructure. This cluster had an estimated  $H_s > 9$  m, and an Average Recurrence Interval (ARI) of 50 years (Bryant and Kidd, 1975). Erosion was recorded in the Garigal estuary at Snapperman and Great Mackerel beaches, and in Kamay along SW-facing BEBs (Congwong, Currewol and Yarra Bay), damaging the newly constructed Port Botany Revetment Wall adjacent to Yarra Bay (Bryant and Kidd, 1975; Foster et al., 1975) (Fig. 1).
- Storm in December 1988 with remarkable rainfall impacted Garigal causing substantial erosion to Great Mackerel (Cowell, 1989; Cowell and Nelson, 1991);

- Cluster of 5 ECLs in June 2007 primarily from SE caused 8 consecutive days of storm waves ( $H_s > 3$  m) and severe coastal erosion on Sydney's open coast beaches (Harley et al., 2016), and on the BEBs at Port Stephens, 230 km north of Sydney (Vila-Concejo et al., 2010) (Fig. 1).
- In June 1998, a powerful storm from E–SE eroded beaches along the NSW coastline (Australian Bureau of Meteorology, 2015).
- Cluster of 3 storms in July 2011 from ESE–SE eroded beaches along the regional coast (Gallop et al., 2020).
- Slow-moving ECL in June 2016 from E-NE when the highest waves  $H_s > 6$  m occurred during spring high tide, causing severe erosion on the open coast (Harley et al., 2017) and at Kamay and Garigal (Gallop et al., 2020) (Fig. 1).

### 3. METHODS

#### 3.1. Image Georeferencing

A total of 67 images were used to form a shoreline timeseries at sub-decadal intervals (Fig. 3). The scale or spatial resolution of the aerial photographs, orthoimages and satellite images are listed in Supplementary Table S2. There were 25 vertical aerial images and 3 satellite images between 1941 and 2017 for Garigal, and 31 vertical aerial images, 1 Orthoimage and 7 satellite images between 1943 and 2017 for Kamay. All images that required geo-rectification in Kamay were georeferenced to a 2014 Orthoimage (Department of Planning, Industry and Environment, NSW Government). As this Orthoimage did not cover the Garigal area, Garigal images were georeferenced to a 2017 satellite image (NearMap Australia Pty Ltd). Standard methodologies were followed, ensuring the highest number of fixed ground control points (GCPs) (Novak, 1992) using permanent fixed features such as buildings, road intersections, jetties and geologic structures. 10–25 GCPs

per image (mean 11) were used depending on image resolution and identifiable features, to perform a 2nd degree polynomial transformation (Rocchini et al., 2012). Root mean square error (RMSE) were calculated and correspond to the sum of residual distances between the location specified for a GCP and the place where it ends up after the transformation (Rocchini et al., 2012). Mean RMSE values were  $3.6 \text{ m} \pm 1.1 \text{ m}$  at Garigal and  $4.5 \text{ m} \pm 2.3 \text{ m}$  at Kamay (study mean =  $3.5 \text{ m} \pm 2.3 \text{ m}$ ) (Supplementary Table S2).

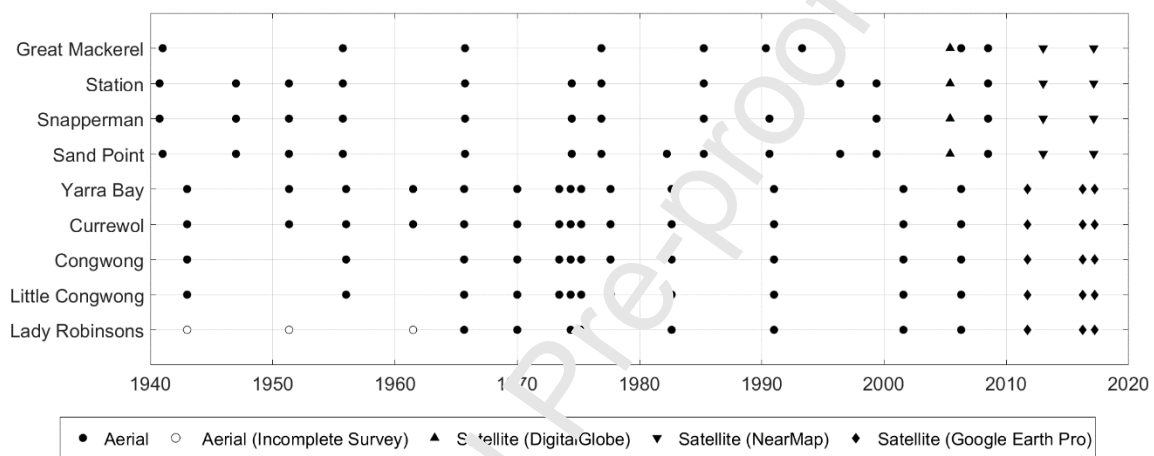


**Figure 3:** Timeseries of aerial and satellite imagery and sources used in this study to track shorelines.

### 3.2. Decadal Shoreline Analysis

This study defined the shoreline as the high-water line (HWL) due to the clear contrast between wet and dry sand in historical images, identified as a consistent shoreline indicator by Boak and Turner (2005). In this region there is limited seasonal shoreline variability for both open coast (Harley et al., 2016) and estuarine beaches (Kennedy, 2002), so infrequent (decadal) images are taken as representative of conditions that year. Uncertainty in shoreline position included an error of 6 m associated with tidal variability, estimated from a mean beach gradient of 10 degrees (Gallop et al., 2020) and spring tidal range of 1.25 m. This is combined with an error of 3 m for onscreen delineation following Ruggiero et al. (2003), and the

study mean RMSE of 3.5 m. The total uncertainty of 7.5 m was calculated following Ruggiero et al. (2003) as the root sum squared of the 3 individual error terms.

Beach width was measured along profiles (2D transects) with origins at the back-beach (seawall or fixed dune toe) to the shoreline identified in each image. The profiles are shore normal and numbered alongshore from north to south (Fig. 1d–g; Table 1). Each of the 41 profiles labelled with P (e.g., P1) in Figure 1 matches Gallop et al. (2020). We also measured 9 groyne profiles labelled with G (e.g., G1) located at the midpoint between groyne pairs along the central and southern sections of Lady Robinsons in Kamay (Fig. 1d). To determine decadal behaviour based on storm erosion and recovery, the BEB recovery timescale  $t_r$  was defined as a function of the amount of sediment eroded during a storm  $E_s$  and the rate of accretion between storms  $A_r$ , and compared with the storm return timescale  $t_{st}$  (observed and also predicted as the AR'). If recovery time  $t_r = E_s/A_r$  then a *quasi-stable* shoreline requires  $t_{st} > E_s/A_r$ .

### 3.3. Offshore wave data

This study used offshore wave data for the Sydney region between 17/07/1987 and 31/07/2017 from a waverider buoy located approximately 10 km offshore, at 90 m water depth (Fig. 1a). The buoy is 22 km south of the Garigal entrance to the open ocean and 30 km north of the Kamay entrance. Hourly measurements of  $H_s$ , maximum wave height ( $H_{max}$ ),  $T_z$ ,  $T_p$  and  $\theta$  were processed to provide daily and 7-day moving averages. Deep-water wave power ( $P$ ) was calculated following Komar (1998) as:

$$P = EC_g \quad (1)$$

where wave energy ( $E$ ) is expressed as

$$E = \frac{1}{16} \rho g H_s^2 \quad (2)$$

where  $\rho$  is seawater density (1025 kg/m<sup>3</sup>),  $g$  is gravitational acceleration (9.81 m/s<sup>2</sup>), and wave group velocity ( $C_g$ ) is expressed as

$$C_g = \frac{gT_z}{2\pi} n \quad (3)$$

where deep-water  $n$  is 0.5. Storms were identified using a Peaks-Over-Threshold method described in Harley (2017) using  $H_s = 3$  m, for a minimum on 6 hours (Shand et al., 2010). Finally, based on storm wave direction (available since 03/03/1992) and entrance orientation the overall estuary exposure to storms was determined as the number of storms that had wave directions that allowed direct propagation through the ocean entrance and into the bay.

## 4. RESULTS

### 4.1. Storm wave exposure

There were 481 storms measured by the offshore buoy between 1987 and 2017; 427 of which occurred between 1992 and 2017 when wave direction measurements were available (Fig. 4). Mean storm statistics were a duration of 33 hours,  $H_s$  of 3.55 m,  $T_z$  of 7.6 s,  $T_p$  of a 10.8 s,  $\theta$  of 158° and storm power of 1350 Kw/m (Fig. 4). Over the thirty years, 380 storms (89%) had waves that could propagate through the Kamay entrance, which faces SE (~135 degrees) and is 1.1 km wide, giving a mean annual storm-exposure rate of 14.5 storms/year (Fig. 5). In comparison, only 37 storms (9%) storms could propagate through the Garigal estuary entrance, which faces N-NE (~25 degrees) and is 1 km wide, giving a mean annual storm-exposure rate of 1.5 storms/year. Therefore, BEBs inside Kamay are potentially exposed to 10 times more storm waves than in Garigal (Fig. 5).

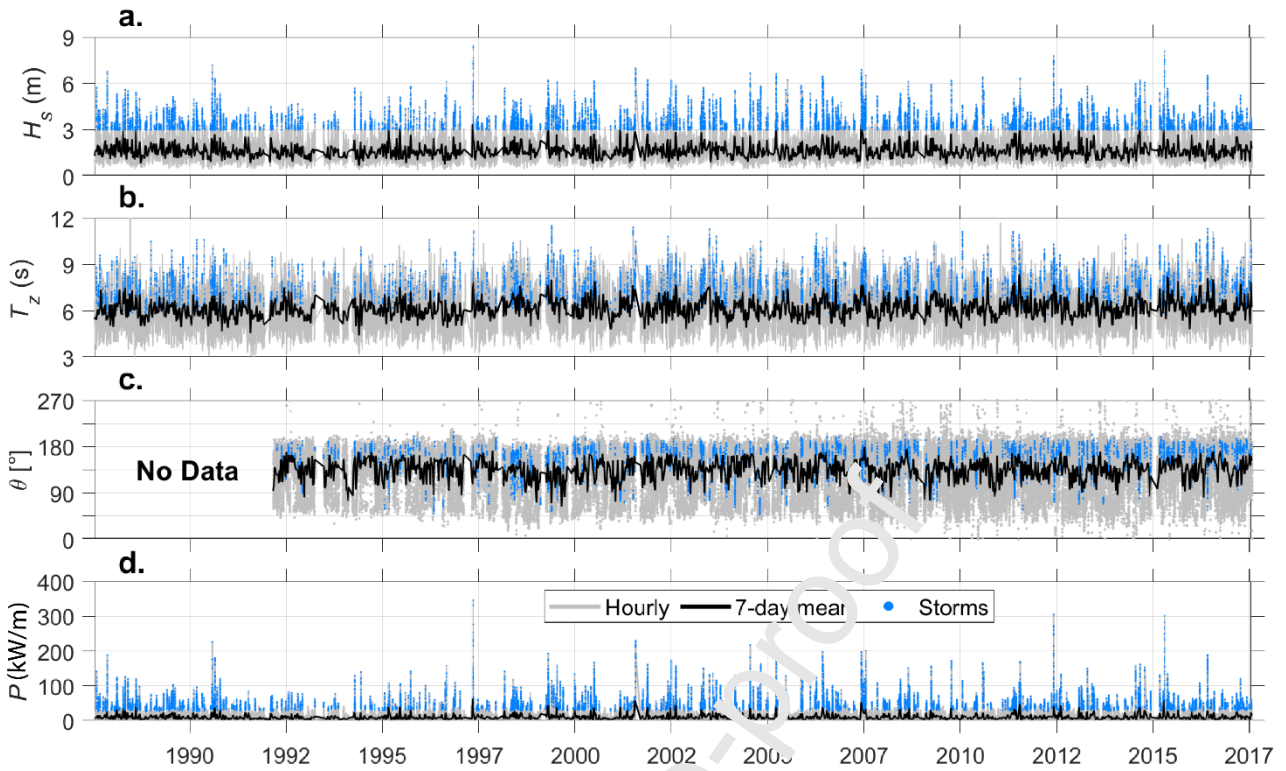


**Figure 4:** Sydney offshore wave data from 1987 to 2017, hourly (grey), 7-day mean (black) and storms (light blue) measurements. (a) Significant wave height ( $H_s$ ), (b) wave period ( $T_z$ ), (c) mean wave direction ( $\theta$ ) and (d) wave power energy flux ( $P$ ).

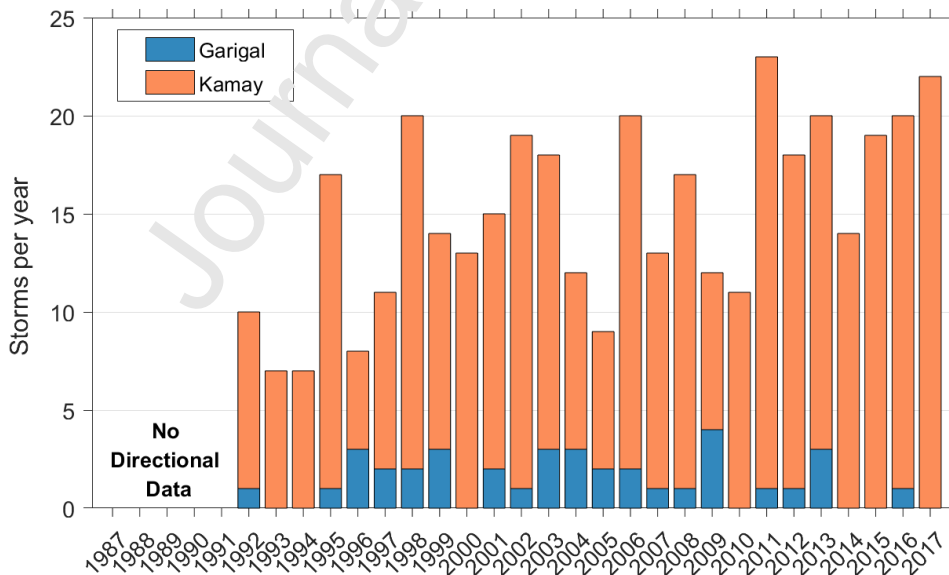


**Figure 5:** Number of storm events per year with storm wave directions that could pass directly through the entrances of Garigal (blue) and Kamay (orange).

## 4.2. GARIGAL SHORELINE ANALYSIS

### 4.2.1. Western Shore: Great Mackerel

Great Mackerel is the most swell-exposed BEB in Garigal, being near the entrance and on the western shore in-line with the entrance (Fig. 1f). This beach exhibited the greatest decadal variability in beach width of the four Garigal BEBs (Fig. 6a; Fig. 7a). Following the 1974 storm cluster, beach width was reduced up to 18 m (39% pre-storm beach width) and the northern creek inlet (adjacent to P1) migrated ~100 m south towards P2 (Fig. 6a). These storms permanently narrowed the beach at P2 (by up to 40 m), from a maximum in the mid-1950s. A storm in late 1988 again reduced width by up to 19 m (53% beach width) and substantial localised flooding was recorded (Supplementary Table S1). Following this, the beach continued to narrow, decreasing by 15 m in the 1990s, 10 m in the early 2000s (Fig. 6a; Fig. 7a) then a further 8 m (< 67% beach width), aided by storms in 2007, 2012 and 2016. Some recovery occurred between storms: almost complete recovery occurred 11 years ( $t_r$ ) after 1974 storms ( $t_{st} = 14$  years), while only partial recovery occurred following the 1988 storm ( $t_{st} = 10$  years) and after the 2011 storms ( $t_{st} = 5$  years) (Fig. 7a). The general trend at Great Mackerel was a net loss between 1941 and 2017 as the recovery timescale ( $t_r$ ) was typically longer than the storm return timescale ( $t_{st}$ ) – widths decreased up to 33 m (mean 0.24 m/year), faster at north (P2) and south (P5–P6) ends than mid-beach (P3) (Fig. 7a; Table 2). Note that the shoreline at P1 is not included in the analysis as it is significantly affected by fluvial processes associated with the proximal creek mouth.

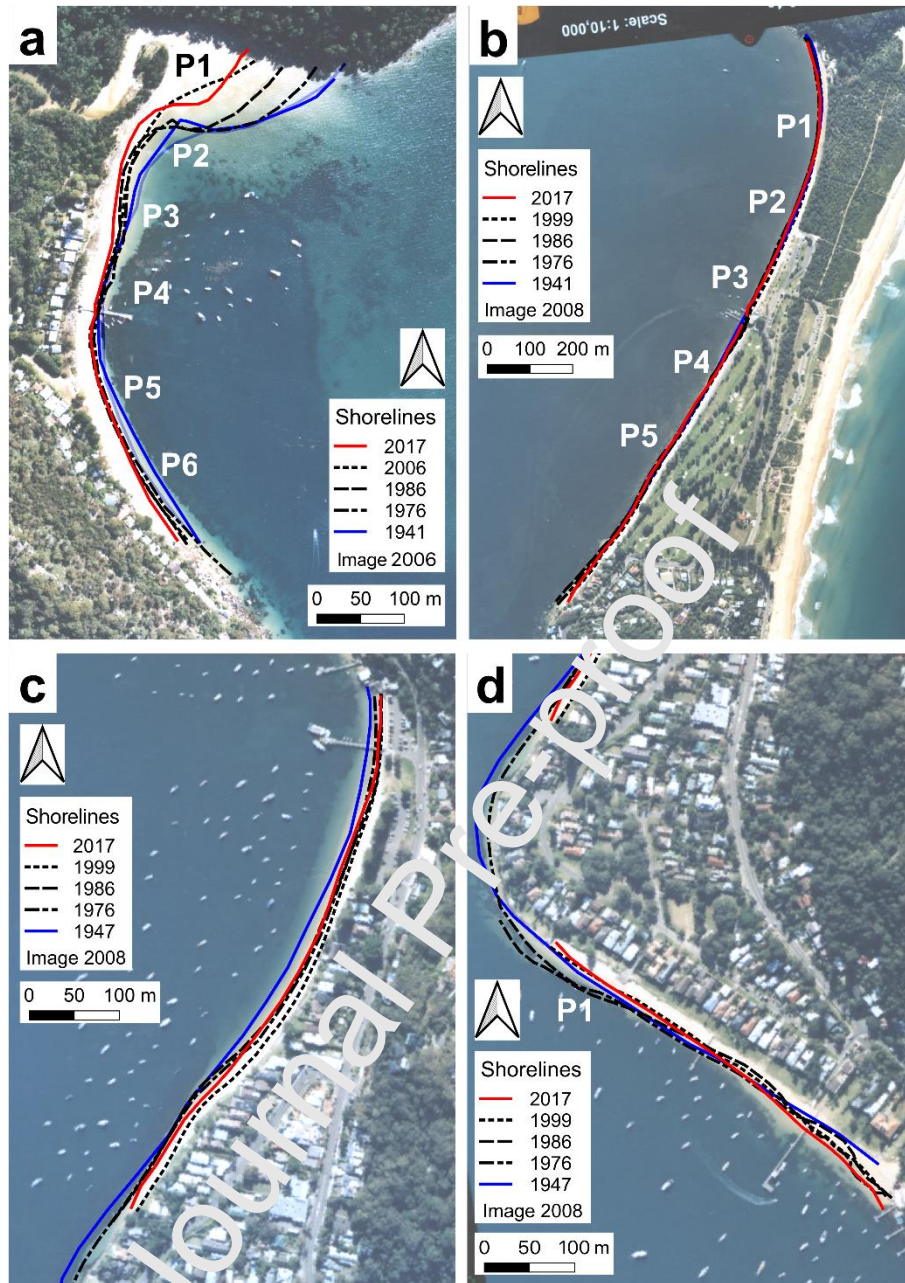


**Figure 6:** Garigal B $\bar{E}$ s (a) Great Mackerel, (b) Station, (c) Snapperman and (d) Sand Point showing the first, last and ~10 yearly shorelines, with beach profiles labelled. Image year is listed in each legend. Note that P1 at Great Mackerel is not included in analysis.

#### 4.2.2. Eastern Shore: Station, Snapperman and Sand Point

Station Beach is a backbarrier beach and the closest to the ocean entrance on the eastern shore of Garigal (Fig. 1g; Fig. 6b; Fig. 7b). Shoreline erosion of up to 8 m (40% of the pre-storm beach width) occurred in the early 1950s, up to 12 m (55% of

the pre-storm beach width) in 1974, and up to 11 m (42% of the pre-storm beach width) in 1998. The 2007, 2011 and 2016 storms also caused BEB erosion (Fig. 6b; Fig. 7b). Notably, recovery took 5 years ( $t_r$ ) following the 1950s storms ( $t_{st} = 24$  years), 3 years ( $t_r$ ) following the 1974 storms ( $t_{st} = 14$  years) and up to 10 years ( $t_r$ ) following the 1998 storm ( $t_{st} = 9$  years) (Fig. 7b). Thus the overall net change in beach width for P1–P4 was negligible (within error) with the typical recovery timescale ( $t_r$ ) shorter or equal to storm return timescale ( $t_{st}$ ). In contrast to this quasi-stable behaviour for P1-P2, the southern end at P5 increased width by 18 m (0.23 m/year) over the same period (Fig. 7b; Table 2).

Similarly, Snapperman Beach widths have not changed much over the decades (Fig. 1g; Fig. 6c; Fig. 7c). Between 1955 and 1974 the beach width reduced by up to 23 m (P3–P5) (Fig. 7c). Following this the central and south beach widths were reduced by up to 11 m (22% of the pre-storm beach width) in 1974. The beach width was reduced by up to 18 m (72% of the pre-storm beach width) in 1998 storm, but the 2007, 2011 and 2016 storms showed negligible erosion (Fig. 6c; Fig. 7c). Recovery took 5 years ( $t_r$ ) following the 1950 storms ( $t_{st} = 24$  years), 3 years ( $t_r$ ) following the 1974 storms ( $t_{st} = 14$  years), was incomplete following the 1988 storm ( $t_{st} = 10$  years), and 10 years ( $t_r$ ) following the 1998 storms ( $t_{st} = 10$  years) (Fig. 7c). Thus, again the overall net change in beach width was negligible at central-beach profiles P3–P5; the recovery timescale ( $t_r$ ) was typically shorter or comparable to storm return timescales ( $t_{st}$ ). This is not true at the northern end (P1–P2) where width has been reduced up to 17 m over the past several decades (0.22 m/year) (Fig. 7c; Table 2).

**Table 2:** Net BEB width change (m) and rate of change in parentheses (m/year) between 1941 (Garigal)/1943 (Kamay) and 2017 and before (\*) and after groyne construction (\*\*). Bold values relate to changes that exceed uncertainty ( $\pm 7.5$  m) and positive values indicate beach widening. The superscript '†' denotes change from 1965 (first image) at Lady Robinsons G8–9.

	BEB	P1	P2	P3	P4	P5	P6	
Garigal	Great Mackerel Station	-	<b>-33.0 (-0.43)</b>	<b>-19.0 (-0.25)</b>	-5.0 (-0.07)	<b>-11.0 (-0.14)</b>	<b>-24.0 (-0.32)</b>	
	Snapperman	<b>-11.0 (-0.14)</b>	<b>-17.0 (-0.22)</b>	-6.0 (-0.08)	-4.0 (-0.05)	-4.0 (-0.05)	-	
	Sand Point	4.0 (0.05)	7.0 (0.09)	<b>12.0 (0.16)</b>	<b>22.0 (0.29)</b>	<b>29.0 (0.38)</b>	-	
	Yarra Bay	-4.8 (-0.06)	<b>30.3 (0.41)</b>	<b>61.1 (0.83)</b>	<b>51.3 (0.69)</b>	-	-	
Kamay	Currewol	<b>-29.0 (-0.88)*</b>	<b>16.4 (0.50)*</b>	<b>59.5 (1.80)*</b>	<b>8.1 (0.25)*</b>	-	-	
		<b>17.1 (0.42)**</b>	3.6 (0.09)**	1.0 (0.02)**	<b>41.6 (1.01)**</b>	-	-	
	Congwong Little	<b>-11.5 (-0.16)</b>	0.8 (0.01)	-2.1 (-0.03)	<b>-1.5 (-0.18)</b>	<b>-7.8 (-0.11)</b>	-	
		<b>-15.8 (-0.48)*</b>	<b>-30.9 (-0.93)*</b>	<b>-9.1 (-0.28)*</b>	<b>-3.9* (-0.27)</b>	3.1 (0.09)*	-	
	Lady Robinsons (Profiles)	-1.6 (0.04)**	2.8 (0.07)**	5.0 (0.12)**	<b>-5.0** (-0.14)</b>	<b>-5.3 (-0.13)**</b>	-	
		<b>10.6 (0.14)</b>	<b>10.8 (0.15)</b>	<b>10.3 (0.14)</b>	-	-	-	
	Lady Robinsons (Groyne)	2.3 (0.03)	1.9 (0.03)	3.2 (0.04)	-	-	-	
		<b>59.8 (0.81)</b>	<b>15.9 (0.22)</b>	<b>3.8 (0.05)</b>	<b>24.5 (0.33)</b>	<b>10.4 (0.14)</b>	<b>10.0 (0.14)</b>	
			<b>G1</b>	<b>G2</b>	<b>G3</b>	<b>G4</b>	<b>G5</b>	<b>G6</b>
			<b>12.9 (0.17)</b>	5.8 (0.08)	<b>-13.2 (-0.18)</b>	5.0 (0.07)	<b>-8.9 (-0.12)</b>	<b>-11.1 (-0.15)</b>
		<b>-9.0 (-0.14)*</b>	<b>-25.4 (-0.41)*</b>	<b>-10.2 (-0.16)*</b>	-2.9 (0.05)*	-2.3 (-0.04)*	<b>-14.7 (-0.27)*</b>	
		2.5 (0.21)**	<b>-11.9 (-0.99)**</b>	<b>-30.1 (-2.51)**</b>	<b>-21.4 (-1.79)**</b>	<b>-13.9 (-0.69)**</b>	<b>-18.2 (-0.91)**</b>	
		<b>G7</b>	<b>G8</b>	<b>G8</b>	-	-	-	
		<b>-21.0 (-0.28)</b>	<b>-24.9 (-0.4)</b> †	<b>31.7 (0.61)†</b>	-	-	-	
		<b>24.2* (-0.45)*</b>	<b>-15.4 (-0.4)</b> †*	<b>8.2 (0.26)†*</b>	-	-	-	
		<b>-5.4* (-0.27)**</b>	<b>-4.1.8 (-0.04)**</b>	2.6 (0.13)**	-	-	-	

Sand Point is the beach furthest (~2.7 km) from the Garigal ocean entrance (Fig. 1g). Despite this, there was a significant shoreline response to storms (Fig. 6d; Fig. 7d). This beach was impacted by the 1950 storm cluster when the beach rotated clockwise, increasing width by 8 m (20% beach width) in the south (P5) (Fig. 7d). The 1974 storms reduced widths along the entire beach, by up to 12 m (29% of the pre-storm beach width). The beach width was then stable from the late-1970s until the 1998 storms when beach widths were reduced by up to 8 m (16% of pre-storm beach width) and again in 2011 by up to 11 m (100 % of pre-storm beach width) at the north end (Fig. 7d). Unlike the other Garigal beaches, beach width was not noticeably impacted by the storms in 1988, 2007 or 2016. Beach recovery took up to

5 years ( $t_r$ ) following the 1950 storms ( $t_{st} = 24$  years), 3 years ( $t_r$ ) following the 1974 storms ( $t_{st} = 14$  years) and recovered after the 2011 storms before the 2016 storm ( $t_{st} = 5$  years) (Fig. 7d). Overall, Sand Point was stable with a recovery timescale ( $t_r$ ) shorter or equal to storm return timescale ( $t_{st}$ ), however the shoreline rotated clockwise: at northern end (P1–P2) width was constant, while at central and southern sites (P3–P5) it prograded by 29 m (0.38 m/year) (Fig. 7d; Table 2).

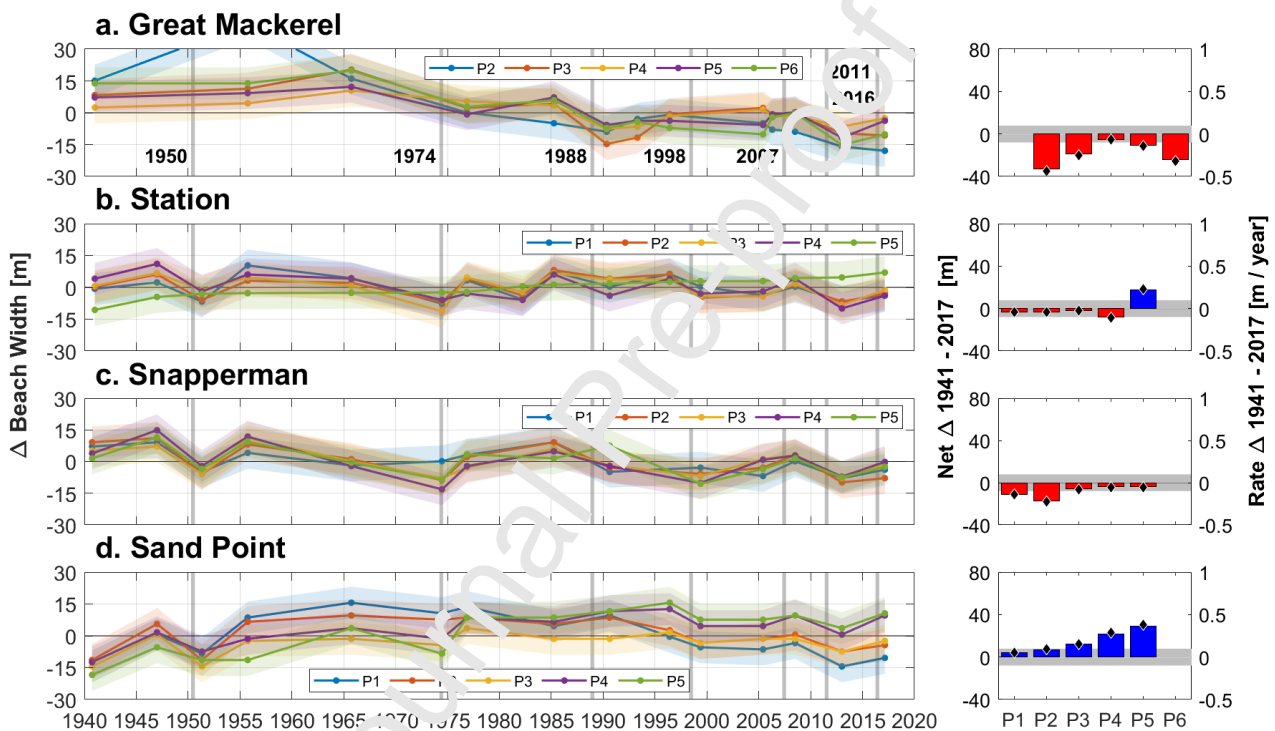


**Figure 7:** Left panels: timeseries of beach width (difference from mean) at (a) Great Mackerel, (b) Station, (c) Snapperman and (d) Sand Point. Right panels: net change in beach width (m) between 1941 and 2017 is shown as increase (blue) or decrease (red), and annual rates of change (m/year) shown as black diamonds. The shaded areas in all plots represent the total uncertainty (7.5 m) and notable storms are shown by the vertical grey lines (Supplementary Table S1).

### 4.3. KAMAY SHORELINE ANALYSIS

#### 4.3.1. Northeast Shore: Yarra Bay, Currewol, Congwong and Little Congwong

Yarra Bay on the northeast shore of Kamay, adjacent to the Port Botany Revetment Wall, exhibited notable decadal variability (Fig. 1e; Fig. 8a; Fig. 9a). In the 1940s the southern half of the Yarra embayment (P3–P4) had limited or no sediment with underlying rocks exposed; in comparison, the northern beach (P1–P2) had ample sediment (Fig. 8a). By the 1960s the beach had started to accrete at the southern end, although some rocks were still exposed between P3 and P4. By the mid-1970s, following dredging for the port and the 1974 storms, the beach underwent extreme erosion at the northern end (P2), with widths reduced by up to 23 m (90% of the pre-storm beach width) and erosion encroached into the dunes (Fig. 2; Fig. 9a). These impacts led to clockwise shoreline rotation, with the northern end narrowing and the southern end widening (Fig. 9a). Following the damaging 1974 storms ( $t_{st} = 14$  years) the beach recovered ( $t_r$ ) partially in the 2 years (P1) prior to the groyne construction and sand nourishment in 1976 (Fig. 2; Fig. 9a). Other notable storm erosion and recovery responses were masked by anthropogenic interventions and a recovery timescale ( $t_r$ ) following these interventions that was shorter or equal to storm return timescale ( $t_{st} > 4$  years) for the 1998, 2007 and 2011 storms (Fig. 8a). The overall trend (1943–2017) was accretional with widths increasing by up to 60 m (0.83 m/year) closest to the groyne (Fig. 8a; Table 2).

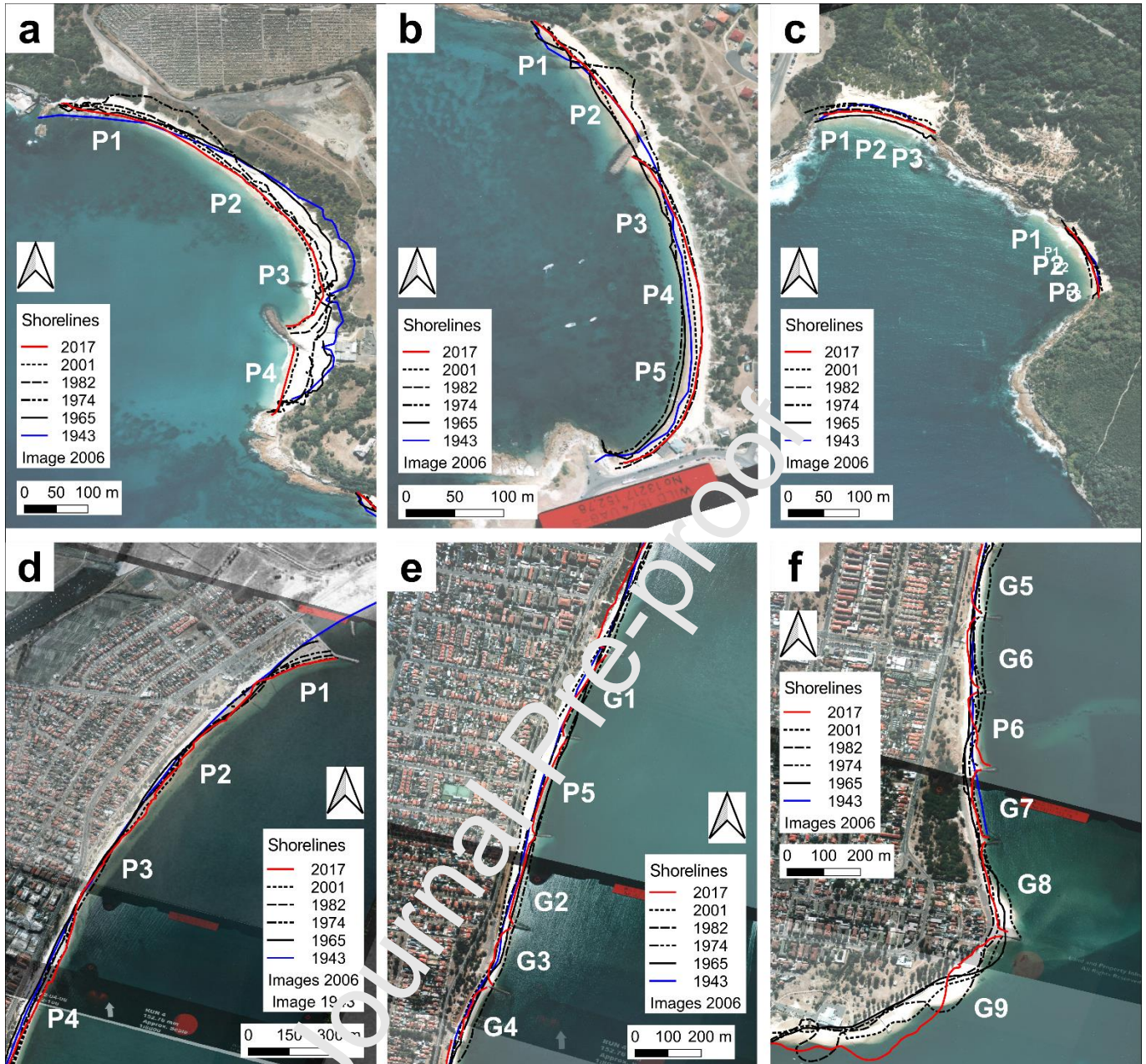


**Figure 8:** Decadal shorelines in Kamay with the first, last and ~10 yearly shorelines are shown, and profiles are labelled. (a) Yarra Bay, (b) Currewol, (c) Congwong (left) and Little Congwong (right), Lady Robinsons North (d), Central (e) and South (f). The red squares are watermarks and image year is listed in each legend

At Currewol, the northern end (P1–P3) is more exposed to waves propagating through the entrance and exhibited larger changes in beach width than the more-sheltered southern end (P4–P5) (Fig. 1e; Fig. 8b; Fig. 9b). Following storms in the early 1950s beach widths were reduced by up to 12 m (61% of the pre-storm beach

width), while following the 1974 storms the shoreline rotated clockwise from P1 to P5 with the northern profiles narrowing by up to 20 m (211% of the pre-storm width) and caused expansive erosion to the dunes (Fig. 9b). There was limited or no recovery in the following 2 years (Fig. 8b). This prompted the construction of a groyne and nourishment in 1976, similar to Yarra Bay (Fig. 2). The beach was stable after these interventions, until the 2007 and 2011 storm clusters combined reduced widths up to 9 m (38 % of pre-2007 storms beach width). Recovery of the groyned beach typically took less than the minimum  $t_{st}$  of 4 years (Fig. 9b). Overall changes in beach width (1943–2017) saw the northern (P1) and central-southern beach (P4) reduced up to 13 m (-0.18 m/year), while the centre beach (P3) was negligible (Fig. 9b; Table 2) suggesting recovery timescale ( $t_r$ ) is shorter or equal to storm return timescale ( $t_{st}$ ).

Congwong and Little Congwong are the most exposed BEBs in Kamay and shorelines at both beaches showed little change, fluctuating by  $\pm 10$  m with recovery timescale ( $t_r$ ) shorter or equal to storm return timescale ( $t_{st}$ ) (Fig. 1e; Fig. 8c; Fig. 9c–d). Congwong was not impacted by the 1974 storms, while Little Congwong accreted by up to 12 m (70% pre-storm beach width) following the storms and its shoreline rotated clockwise from north to south (Fig. 9c–d). The 1950, 1998, 2007, 2012 and 2016 storms caused negligible responses. Following the 1974 storms, Little Congwong returned to pre-storm widths within a year faster than the shortest storm return time ( $t_{st}$ ) of 4 years in this study (Fig. 9c–d). The overall trend (1943–2017) at Congwong had widths increased up to 10 m (0.14 m/year), while at Little Congwong net change was negligible (Fig. 9c–d; Table 2).

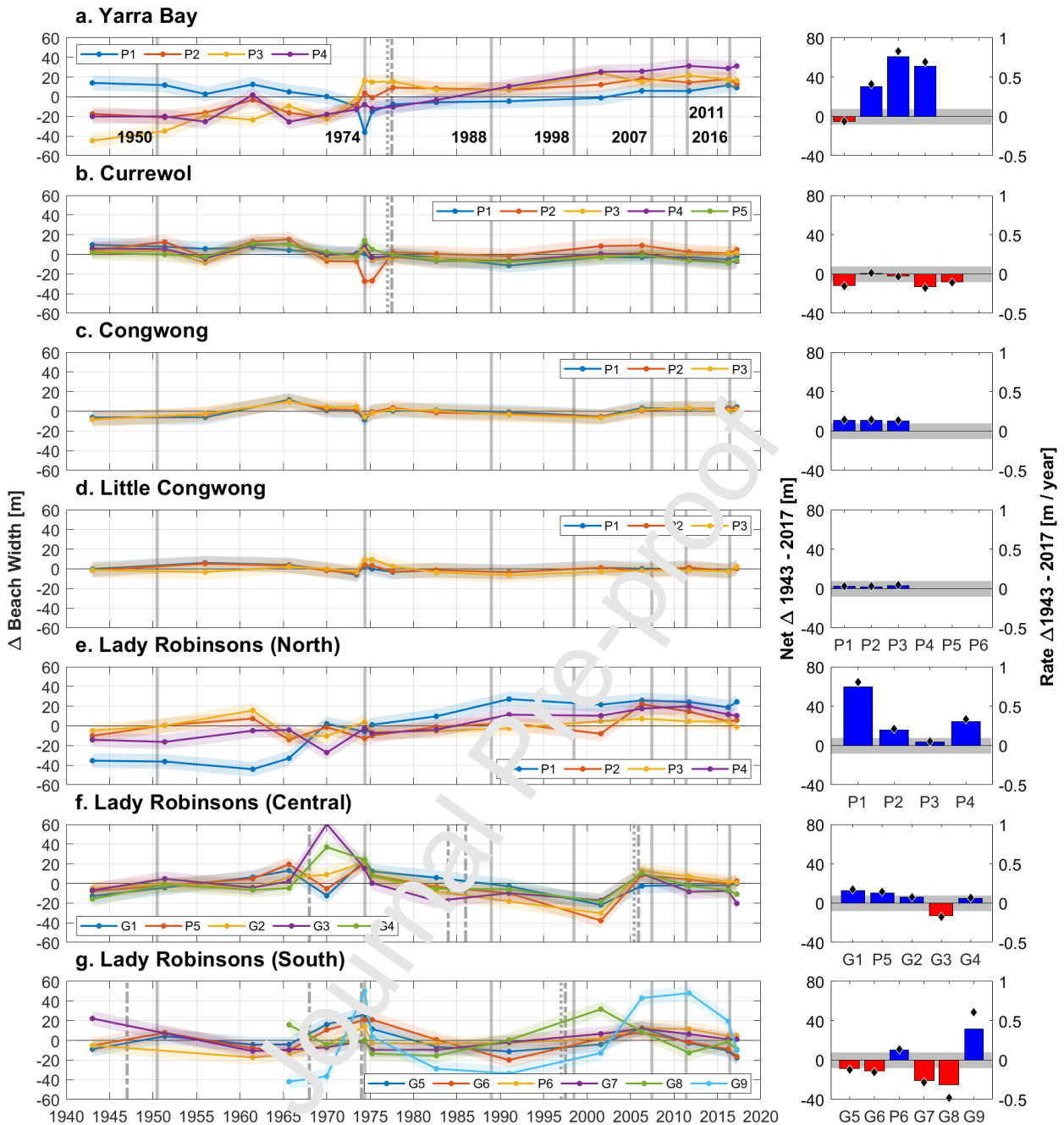


**Figure 9:** Left panels: timeseries of beach width (difference from mean) for (a) Yarra Bay, (b) Currewol, (c) Congwong, (d) Little Congwong and Lady Robinsons north (e), central (f) and south (g). Right panels: net change in beach width (m) between 1943 and 2017 with net increase (blue) or decrease (red), and rates of change (m/year) shown as black diamonds. Note the shaded areas in both the left and right plots represent the total uncertainty (7.5 m). Notable storms are denoted by solid grey lines (Supplementary Table S1), groyne construction by grey dotted lines, and sand nourishment by grey dot-dash lines. The net rates for G8 and G9 in (g) were calculated between 1965 (first image) and 2017.

#### 4.3.2. Western Shore: Lady Robinsons

Lady Robinsons is the farthest from the estuary entrance (8.2 km) and has been altered the most by anthropogenic interventions (Fig. 1d; Fig. 9e–g). There were significant differences in shoreline behaviour between the northern, central and southern sections. The northern section (P1–P4) accreted overall (1943–2017) with beach widths increasing by up to 60 m (0.81 m/year), while the shoreline rotated clockwise P1 to P4 (Fig. 8d; Fig. 9e; Table 2). The 1974 storm cluster impacted the beach (P3) narrowing it by 10 m (44% of the pre-storm width) (Fig. 9e). The northern profiles affected by these storms did not recover to pre-1974 widths until 1990 – much longer than the 14-year storm return time ( $t_{st}$ ). However, subsequent storms did not impact this section due to the airport runway extensions that extend 2.4 km SW into the bay (Fig. 1; Fig. 2; Fig. 9e).

The beach widths on the central section of Lady Robinsons (P5, G1–G4) continually narrowed due to storms and anthropogenic modifications in the bay (Fig. 1d; Fig. 9f). This section was eroded following the 1974 storms by 11 m (19% pre-storm beach width) and then continued to lose sand coinciding with dredging for a second runway that protrudes SW into bay in the 1990s (Fig. 1; Fig. 2); these losses were reversed when groynes were constructed in 2005 (Fig. 8e; Fig. 9f). The 2007 and 2011 storm clusters and the 2016 storm further eroded this section with limited recovery recorded by the end of this study, suggesting recovery timescales ( $t_r$ ) are longer than the 4-to-5-year storm return timescales ( $t_{st}$ ) for these storms (Fig. 9f). Although the storms and dredging reduced beach widths, repeated sand nourishment increased the net beach width (1943–2017) up to 12.9 m/year (0.17 m/year), except at G3 which had overall width reduced by 13.2 m/year (0.18 m/year) (Fig. 2; Fig. 9f; Table 2).

Beach widths in the southern section (P6, G5–G9) were characterised by large shoreline fluctuations and decadal shoreline retreat that were mitigated by four sand nourishment interventions in 1943, 1964, 1971 and 1997 (Fig. 1d; Fig. 2; Fig. 9g). The 1974 storms reduced beach width by up to 17 m (80% of the pre-storm beach width) with only one profile recovering 15 years later (G8) (Fig. 9g). Groynes were built in 1997 to stabilise this section, however the 2007, 2011 and 2016 storms again eroded this section with no recovery between storms, suggesting recovery timescales ( $t_r$ ) in this section were longer than the 14-year storm return timescale ( $t_{st}$ ) following the 1974 storm (Fig. 9g). Shorelines between the groynes had anti-clockwise orientations (Fig. 8f), indicating southward longshore transport. Overall change in beach width (1943–2017) was most varied at southern sites that are influenced by tidal currents at the mouth of Tucoerah, with the southernmost site (G9) accreted 30 m (0.61 m/year) while the adjacent beach (G8) eroded by 24.9 m (-0.48 m/year) (Fig. 8f; Table 2).

## 5. DISCUSSION

### 5.1. Decadal behaviour of BEB shorelines

Considerable erosion of the subaerial BEBs occurred during storms when ocean swell waves propagated through the entrances of semi-enclosed estuaries – specifically at BEBs proximal to sediment sinks and altered by anthropogenic interventions. During low-energy wave conditions between storms, transport of sand back onto beaches was slow and post-storm recovery took years. In previous work (Costas et al., 2005; Gallop et al., 2020; Harris et al., 2020; Nordstrom and Jackson, 2012), incomplete recovery in width was observed over months to several years, while this study shows that some BEBs can recover fully after storms, given enough time (Fig. 9c, f and 10). While the return time of storms is similar within a given

estuary, these data show that the recovery time is related to the distance of each BEB from estuary entrance as this influences the modal wave energy between storms (which modulate both drift and swash accretion processes). When storms occur frequently or at beaches where recovery time is slow, the recovery timescale ( $t_r$ ) will be longer than the storm return timescale ( $t_{st}$ ) and recovery will be incomplete. The results include BEB shorelines where  $t_r > t_{st}$  and others where  $t_r < t_{st}$  or  $t_r \sim t_{st}$ , representing different decadal-scale behaviours (Fig. 7; Fig. 9; Fig. 10). Based on the BEBs in this study (Fig. 10; Table 3), we propose a decadal behavioural typology of BEB shorelines: *prograding*, *quasi-stable*, *retreating* and *storm relict* BEBs. Where  $t_r < t_{st}$ , beaches recover between storms as they do on the open coast and these *quasi-stable* BEBs show limited decadal-scale change. They may occur where beaches are entirely sheltered from storm waves (Currewoll post-1974) or exposed to significant wave energy between storms and available sediment sources (e.g., Congwong and Little Congwong, Fig. 9b–c). This supports Costas et al. (2005) who suggest that wave exposure is vital for any beach recovery. However, where  $t_r > t_{st}$ , beaches cannot recover before the next erosion event and these *retreating* BEBs exhibit partial recovery between storm events (e.g., Great Mackerel). Some beaches exhibited negligible recovery between storms (Table 3) – these *storm relict* BEBs (e.g., Lady Robinsons south) appear unrelated to modal conditions and reflect prior storm erosion. These BEBs may have formed under different environmental conditions and, without further intervention, could eventually disappear under contemporary conditions. Finally, *prograding* BEBs were also observed (e.g., Sandy Point, Lady Robinsons north). Although the mechanisms and sediment sources for this behaviour are unknown (Gallop et al., 2020), reduced swell exposure (far removed from ocean entrance), fluvial sources and alongshore

transport are likely factors in this progradation (Fig. 7d; Fig. 9d). As for *storm relict* BEBs, these *prograding* BEBs may also reflect environmental change (i.e., local sediment budget has been altered).

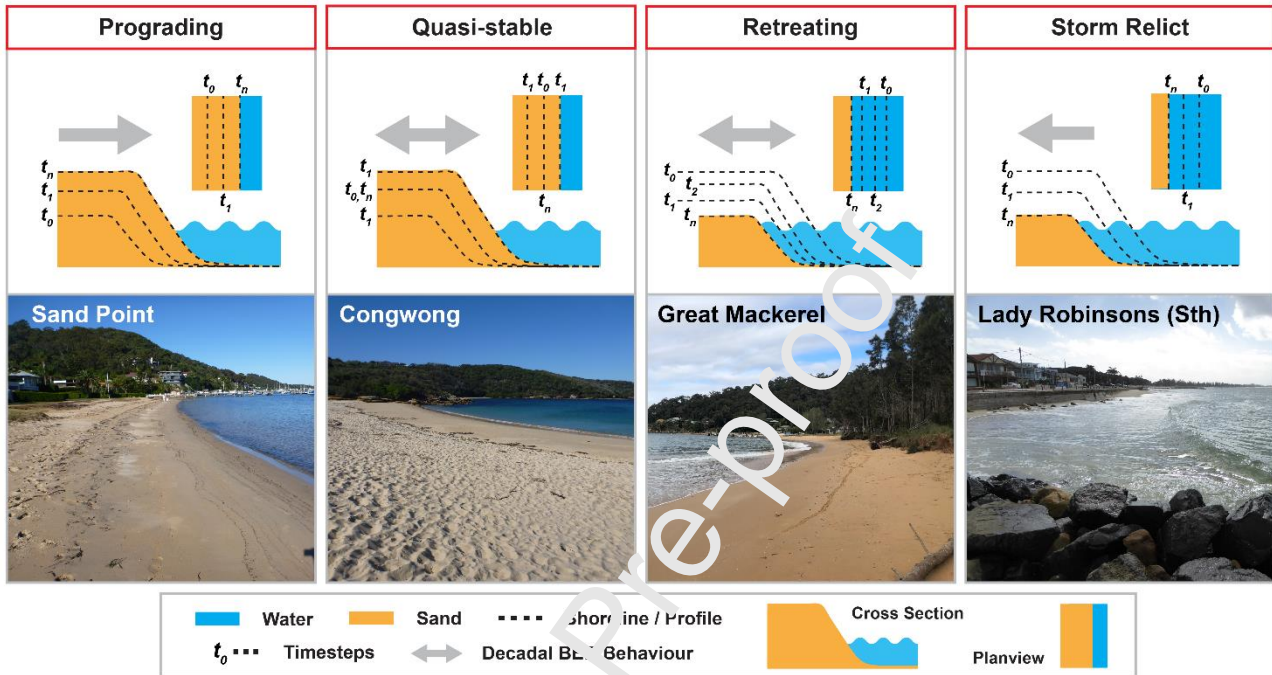


**Figure 10:** A decadal behavioural typology for BEBs. *prograding*, *quasi-stable*, *retreating*, and *relict*. Behaviours are shown with an example BEB from Garigal or Kamay.

A key finding is that BEB shoreline recovery can be absent or slower than open-coast beaches, which is typically within 3 years for the subaerial beach following extreme storms in this region (Harley et al., 2016). If we note that recovery time  $t_r = E_s/A_r$  where  $E_s$  is amount eroded during storm and  $A_r$  is the rate of accretion between storms, then the requirement for *quasi-stable* beaches is  $t_{st} > E_s/A_r$ . Thus, beaches may start to retreat due to increased storm frequency (smaller  $t_{st}$ ), more severe erosion during storms (larger  $E_s$ ), or slower accretion between storms (smaller  $A_r$ ). Climate change may alter storm frequency, wave height and incident direction, which then change  $E_s$ . Moreover, local anthropogenic changes like

dredging and structures can alter wave propagation into estuaries/bays, changing both  $E_s$  and  $A_r$ , and nourishment can increase  $A_r$ . More recognition of the influence of anthropogenic impacts alongside the slow-evolution paradigm for BEBs has major implications for the management of estuary and bay shorelines in major cities.

**Table 3:** Decadal behavioural typology of the BEBs in Garigal and Kamay.

	<b>BEB Location</b>	<b>Behaviour</b>	<b>Behaviour after intervention</b>
<b>Garigal</b>	Great Mackerel	<i>Retreating</i> (north/south) <i>Quasi-stable</i> (central)	<i>Retreating</i> (north/south) <i>Quasi-stable</i> (central)
	Station	<i>Quasi-stable</i> (north) <i>Prograding</i> (south)	-
	Snapperman	<i>Retreating</i> (north) <i>Quasi-stable</i> (central/south)	-
	Sand Point	<i>Quasi-stable</i> (north)	-
		<i>Prograding</i> (south)	-
<b>Kamay</b>	Yarra Bay	<i>Storm Relict</i> (north) <i>Quasi-stable</i> (south)	<i>Quasi-stable</i> (all)
	Currewol	<i>Storm Relict</i> (north) <i>Quasi-stable</i> (south)	<i>Quasi-stable</i> (all)
	Congwong	<i>Quasi-stable</i>	-
	Little Congwong	<i>Quasi-stable</i>	-
	Lady Robinsons	<i>Quasi-stable</i> (north)	<i>Prograding</i> (north)
		<i>Storm Relict</i> (central) <i>Storm Relict</i> (south)	<i>Quasi-stable</i> (central) <i>Retreating</i> (south)

## 5.2. Geomorphological influences on decadal BEB evolution

### 5.2.1. Distance from estuary or bay entrance

Distance from the ocean entrance controls BEB responses to and recovery from storms (Fig. 7b; Fig. 9c). BEBs that are close to the entrance present behaviours that are commonly *quasi-stable* (e.g., Congwong and Station); in contrast with *prograding*, *retreating* and *storm relict* behaviours away from the entrance (Fig. 10; Table 3). Costas et al. (2005), Eulie et al. (2017) and Gallop et al. (2020) suggest that exposure to swells and a continuing supply of marine sediment are essential to maintain subaerial volume and BEB shoreline width (Fig. 7b; Fig. 9c). For instance, Kamay has ~10 times the number of storms with waves that enter the estuary

compared to Garigal (Fig. 5). In Kamay, following the 1974 storms, BEBs located near the entrance exhibited rapid recovery, e.g., Congwong recovered in 3 years and was *quasi-stable* compared to Lady Robinsons south which is 6 times further from the entrance and had only partial recovery after 15 years and was *retreating/storm relict*. (Fig. 9c, g; Table 3). Alternatively, BEBs that have *prograding* behaviours (e.g., Sand Point, Lady Robinsons north) may be at the inner limit of swell propagation where waves no longer have energy required to transport beach sediments (Fig. 6d; Fig. 8d; Fig. 10); suggesting that *prograding* BEBs are controlled by tidal, wind-wave, fluvial or other processes that move the sediment onto beaches. For example, Austin et al. (2018) and Vila-Concejo et al. (2020) found that wave energy within estuaries can be refracted/diffracted around headlands, along estuary/bay shores and over tidal shoals and deltas, encouraging alongshore transport onto the subaerial BEBs. Overall, results suggest that entrance adjacent BEBs may be less vulnerable to decadal management issues and more attention may be required for those with less stable behaviours.

### 5.2.2. Flood-tide deltas

A flood-tide delta may act as a source or sink for BEB sediments (Austin et al., 2018; Vila-Concejo et al., 2011). For example, Great Mackerel had a sediment sink (*retreating*) while Snapperman had a sediment source (*quasi-stable*) (Fig. 7a, c). Both of these BEBs are adjacent to the Garigal flood-tide delta but have different behaviours (Table 3) and exposure to swells (Gallop et al., 2020) (Fig. 1). Harris et al. (2020) and Vila-Concejo et al. (2007) indicate that BEB sediments can be transported by storm waves onto flood-tide deltas and sandy tidal shoals, with this sediment loss becoming permanent if sediments are moved below the modal wave base (Austin et al., 2018) or removed by subsequent tidal action. Gallop et al. (2020)

outline the *retreating* behaviour at Great Mackerel (Table 3), suggesting that sediments eroded from the subaerial beach and shoreface post-storm may be transported alongshore or form a subtidal terrace that extends to flood-tide deltas and may be a one-way process where sediment is transported tidally off the shoal and into deeper water. These authors and others (Costas et al., 2005; Jackson, 1995; Nordstrom and Jackson, 2012) state that the limited wave energy under modal conditions can fail to return all eroded BEB sediments. Alternatively, sediments may arrive onto BEBs from nearshore sources (Vila-Concejo et al., 2010; Vila-Concejo et al., 2007) or have travelled along estuary/bay shores from the entrance (Harris et al., 2020). This is evident in Garigal where sediments are transported along the eastern shore along and between Station and Snapperman BEBs (both *quasi-stable*), maintaining the subaerial beach. While Snapperman BEB is adjacent to the flood-tide delta (Fig. 1g; Table 3), subaerial and shoreline erosion is evident on decadal time scales at other sites near the flood-tide delta in Port Stephens in SE Australia (Austin et al., 2018; Harris et al., 2020) as well as adjacent to tidal shoals and tidal channels on back-barrier BEBs in Portugal (Carrasco et al., 2012). Findings from this study suggest source and sink pathways associated with flood-tide deltas are fundamental to contiguous BEBs and thus should be considered in BEB management.

### 5.2.3. River and creek mouths

BEBs adjacent to river or creek mouths are highly dynamic as they are at the intersection of fluvial and tidal processes in addition to the influence of wave-driven processes (Vila-Concejo et al., 2020). These BEBs present a range of decadal shoreline behaviours from *prograding* (e.g., Lady Robinsons north) through to *retreating* (e.g., Great Mackerel) (Fig. 7a; Fig. 9e; Table 3). At Great Mackerel, the

decadal *retreating* behaviour and slow recovery of the subaerial beach (up to 11 years) following the 1974 storms appears to be impacted by the alongshore migration of the creek mouth which narrows beach widths (Fig. 1c; Fig. 6a; Fig. 10). Meanwhile, Cowell (1989) and Gallop et al. (2020) point out that short-term BEB morphodynamics are equally impacted by river or creek mouths, when BEBs lose more sand due to river and creek outputs. Equally, BEBs located in low-lying settings (e.g., Kamay) on the front of sand spits and prograded barriers (e.g., Lady Robinsons south) can represent *retreating* or *storm relict* behaviours due to fluvial processes (Fig. 10). These BEBs can require anthropogenic intervention to stabilise or mitigate BEB shorelines (Fig. 2; Fig. 8g), especially if shorelines are modified (e.g., Lady Robinsons south). Alternatively, shorelines can accrete downdrift if the BEB is dominated by alongshore sediment transport (Nordstrom and Jackson, 2012). At Lady Robinsons north results suggest alongshore transport, the northern river mouth and a retaining wall encourage the decadal *prograding* behaviour (Fig. 2; Fig. 8d). Meanwhile, the variability of the dynamic southern section could be attributed to the proximity to the Tucoerah River which may supply sediment as well as enhance tidal currents and which can dominate morphological change that includes migrating sand bars (see Fig. 8f). The variability of BEB shorelines near river and creek mouths is not driven by wave forcing alone, and dynamical understanding must consider the interaction of fluvial, tidal and wave forcing.

### **5.3. Importance of anthropogenic interventions for BEBs**

BEBs in the same estuary often have different decadal shoreline behaviours (Fig. 10). BEBs with the largest shoreline change are typically those with a history of anthropogenic intervention, for example Currewol and Yarra bay were *storm relict* and post-intervention are *quasi-stable* (Table 3). While at Lady Robinsons,

reductions in beach width are likely due to a sediment sink that developed following dredging in the 1970s and 1990s for the Sydney Airport runways and the port navigation channel (Fig. 2; Fig. 9e–g). Increases to estuary and bay water depth due to dredging, can destabilise shorelines and erode subaerial sediments by modifying waves processes and redirecting swell energy to BEB shorelines and by creating sediment sinks (Austin et al., 2018; Nordstrom, 1992); an example of which is the *retreating* behaviour along central and south Lady Robinsons (Table 3). In the Algarve (Portugal), Carrasco et al. (2012) notes that dredging of nearshore tidal shoals and channels is the primary driver of BEB shoreline retreat, even at locations not exposed to swell waves. Clearly these factors contribute to *retreating* and *storm relict* shoreline behaviours with important management implications.

Anthropogenic interventions to counter decadal shoreline retreat in estuaries and bays include groynes and revetments (Nordstrom and Jackson, 2012). This study and others (Frost, 2011; Lowe and Kennedy, 2016) emphasise how groynes and sand nourishment can mitigate the effects of repetitive storm erosion, alongshore sediment transport, shoreline rotation and increased wave exposure on BEB shorelines (Fig. 8a–b). For instance, at Lady Robinsons there are two phases of groyne construction following bay dredging for the port (1970s) and the airport (1990s) (Fig. 2; Table 3). Yarra Bay and Currewol both display *storm relict* shorelines following the erosion of the 1974 storms and a clockwise shoreline rotation following the construction of the Port Botany revetment in the early 1970s. This highlights how interventions change sediment supply or exposure for adjacent BEBs (Fig. 2; Fig. 9a–b, e–g; Fig. 10). Nordstrom (1992) and Qiao et al. (2018) emphasise how BEBs are vulnerable to anthropogenic interventions, with decadal losses to BEB widths in Hong Kong and in the USA. In Kamay, anthropogenic interventions led to diversion,

refraction and reflection of swell energy onto previously sheltered shorelines in Yarra Bay and Currewol. Both now have a central groyne structure that supports *quasi-stable* behaviours (Table 3). Furthermore, anthropogenic interventions to river and creek mouths can cause *retreating* (Great Mackerel) and *prograding* (Lady Robinsons north) behaviours (Fig. 2; Table 2), as shorelines readjust slowly over decadal scales. Historically, engineering interventions rarely considered BEB shorelines which in many cases (e.g., Lady Robinsons, Yarra Bay) then required subsequent intervention (groynes, sand nourishment) to maintain the shorelines (Fig. 2; Table 3). Future anthropogenic interventions must consider decadal BEB behaviours, to preclude future shoreline retreat.

## 6. CONCLUSIONS

The decadal-scale behaviours of sandy shorelines in natural and heavily modified estuaries in SE Australia have been quantified and analysed in this study. Based on this assessment of 76 years of imagery (1941–2017), a behavioural typology of BEB decadal evolution is presented with four types of BEB: *prograding*, *quasi-stable*, *retreating* and *storm relict* shorelines. *Prograding* BEBs have shorelines (subaerial beach widths) that migrate seaward, *quasi-stable* BEBs present minimal decadal change, *retreating* and *storm relict* BEBs have shorelines that migrate landward with partial or no recovery between storms, respectively. BEBs near the ocean entrance of estuaries and bays are typically swell exposed and *quasi-stable*. They recover at rates comparable to open coast beaches (< 3 years). In contrast, BEBs farther from the entrance exhibit all four behaviours, are less swell exposed and when they recover do so at slower rates (< 15 years) – that commonly exceed storm return timescales. *Prograding* BEBs are typically at a distance from the ocean entrance, swell sheltered and controlled by other processes including fluvial/tidal transport.

BEBs adjacent to a flood-tide delta can present *quasi-stable* or *retreating* behaviours depending whether the delta acts as a sediment source or sink, respectively. Decadal behaviours are the most variable on BEBs adjacent to river and creek mouths due to the interaction of fluvial and marine processes, alongshore transport and anthropogenic intervention (e.g., groynes and revetment, sand nourishment, dredging). Dredging and land reclamation can lead to *retreating* and *storm relict* shorelines if new sediment sinks are created and if wave energy is redirected through dredged channels to previously protected BEBs. Meanwhile, groynes and sand nourishment are measures that can be successful in creating *quasi-stable* BEB, if interventions consider the altered wave or sediment conditions within a modified estuary or bay. Future research should focus on the impacts of wave propagation, sediment sources and local transport patterns within natural and modified estuaries and bays.

## 7. ACKNOWLEDGEMENTS

We acknowledge the traditional custodians of the Aboriginal lands on which this research was conducted. Thanks to the NSW Department of Planning, Industry and Environment (DPIE) and the Newcastle Region Library for supplying historical aerial images, to Manly Hydraulics Laboratory (DPIE) for supplying wave data, and to David M. Kennedy from the University of Melbourne for Garigal NearMap images. AVC and JLL are grateful for support received through the Partnership Collaboration Award linking the University of Sydney with University of California Davis.

## 8. DATA AVAILABILITY

The aerial and satellite image and major storm details are available in the supplementary information, while the shoreline datasets reported in the paper are available from the corresponding author on reasonable request.

## 9. REFERENCES

- Aijaz, S., Treloar, D., 2003. Beach management options at Lady Robinsons Beach, Botany Bay, Australia, *Oceans 2003. Celebrating the Past ... Teaming Toward the Future* (IEEE Cat. No.03CH37492), pp. 238-245 Vol.231.
- Austin, T., Vila-Concejo, A., Short, A., Ranasinghe, R., 2018. A Multi-Scale Conceptual Model of Flood-Tide Delta Morphodynamics in Micro-Tidal Estuaries. *Geosciences*, 8(9), 324.
- Australian Bureau of Meteorology, 2015. *Stormy Weather: A century of storms, fire, flood and drought in New South Wales*, Australian Government, pp. 29-30.
- Birkemeier, W.A., Nicholls, R.J., Lee, G.-h., 1979. Storms, storm groups and nearshore morphologic change, *Coastal Sediments*. ASCE, pp. 1109-1122.
- Boak, E.H., Turner, I.L., 2005. Shoreline Definition and Detection: A Review. *Journal of Coastal Research*, 688-703.
- Bryant, E.A., Kidd, R., 1975. Beach erosion, May-June, 1974, Central and South Coast, NSW.
- Carrasco, A.R., Ferreira, Ó., Matias, A., Freire, P., 2012. Natural and human-induced coastal dynamics at a back-barrier beach. *Geomorphology*, 159-160, 30-36.
- Costas, S., Alejo, I., Vila-Concejo, A., Nombela, M.A., 2005. Persistence of storm-induced morphology on a nodal low-energy beach: A case study from NW-Iberian Peninsula. *Marine Geology*, 224(1-4), 43-56.
- Cowell, P.J., 1989. *Advisory Report on Management of Beach Erosion at Mackerel Beach*. Coastal Protection Advisory Service.
- Cowell, P.J., Kannane, A., 2000. *Review of Changes to the Shores and Bed of Botany Bay: Past and Future*. New South Wales Healthy Rivers Commission Occasional Paper 1005.
- Cowell, P.J., Nelson, H., 1991. Management of beach erosion due to low swell, inlet and greenhouse effects: Case study with computer modelling, 10th Australasian Conference on Coastal and Ocean Engineering, Hamilton, New Zealand, pp. 311-315.
- Davies, P.R.E., McIlquham, J.D., 2011. Geotechnical design for the Port Botany expansion project, Sydney. *Proceedings of the Institution of Civil Engineers - Geotechnical Engineering*, 164(3), 149-167.
- Eulie, D.O., Walsh, J.P., Corbett, D.R., Mulligan, R.P., 2017. Temporal and Spatial Dynamics of Estuarine Shoreline Change in the Albemarle-Pamlico Estuarine System, North Carolina, USA. *Estuaries and Coasts*, 40(3), 741-757.
- Foster, D.N., Gordon, A., Lawson, N., 1975. *The Storms of May-June 1974*, Sydney, NSW, Second Australian Conference on Coastal and Ocean Engineering, 1975: *The Engineer, the Coast and the Ocean*, The Institution of Engineers, Australia, pp. 1.

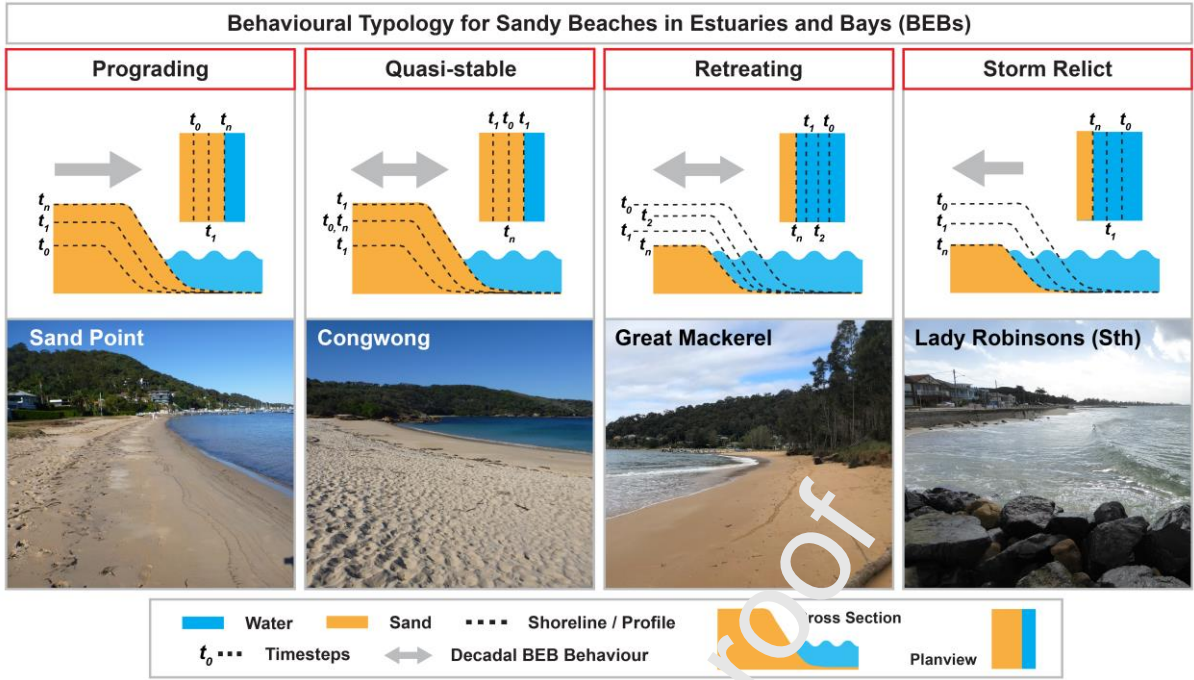
- Frost, G., 2011. Review of Coastal Processes and Evaluation of the Impact of the Constructed Groynes along Lady Robinsons Beach, Botany Bay, New South Wales, Australia. Bachelor of Environmental Science (Honours) <https://ro.uow.edu.au/thsci/17>, University of Wollongong, Wollongong, Australia.
- Gallop, S.L., Vila-Concejo, A., Fellowes, T.E., Harley, M.D., Rahbani, M., Largier, J.L., 2020. Wave direction shift triggered severe erosion of beaches in estuaries and bays with limited post-storm recovery. *Earth Surface Processes and Landforms*, 45(15), 3854-3868.
- Harley, M.D., 2017. Coastal Storm Detection. In: P. Ciavola, G. Coco (Eds.), *Coastal Storms: Processes and Impacts*. Wiley, Chichester, pp. 1-19.
- Harley, M.D., Turner, I.L., Kinsela, M.A., Middleton, J.H., Mumford, P.J., Splinter, K.D., Phillips, M.S., Simmons, J.A., Hanslow, D.J., Short, A.D., 2017. Extreme coastal erosion enhanced by anomalous extratropical storm wave direction. *Scientific Reports*, 7(1), 6033.
- Harley, M.D., Turner, I.L., Splinter, K.D., Phillips, M.S., Simmons, J.A., 2016. Beach response to Australian East Coast Lows: A comparison between the 2007 and 2015 events, Narrabeen-Collaroy Beach. *Journal of Coastal Research*, 388-392.
- Harris, D.L., Vila-Concejo, A., Austin, T., Benavente, J., 2020. Multi-scale morphodynamics of an estuarine beach adjacent to a flood-tide delta: Assessing decadal scale erosion. *Estuarine, Coastal and Shelf Science*, 106759.
- Jackson, N.L., 1995. Wind and Waves. Influence of Local and Non-local Waves on Mesoscale Beach Behavior in Estuarine Environments. *Annals of the Association of American Geographers*, 85(1), 21-37.
- Jones, G., 1981. Effects of dredging and reclamation on the sediments of Botany Bay. *Australian Journal of Marine and Freshwater Research*, 32, 369-377.
- Kennedy, D.M., 2002. Estuarine Beach Morphology in Microtidal Middle Harbour, Sydney. *Australian Geographical Studies*, 40(2), 231-240.
- Komar, P.D., 1998. *Beach Processes and Sedimentation*. Prentice Hall.
- Kulmar, M., Gordon, A., 1987. Coastal Processes of the Pittwater North Western Foreshores, Eighth Australasian Conference on Coastal and Ocean Engineering 1987: Preprints of Papers. Institution of Engineers, Australia, pp. 109.
- Lowe, M.K., Kennedy, D.M., 2016. Stability of artificial beaches in Port Phillip Bay, Victoria, Australia. *Journal of Coastal Research*, 75(sp1), 253-257, 255.
- Nordstrom, K.F., 1992. *Estuarine Beaches: An introduction to the physical and human factors affecting use and management of beaches in estuaries, lagoons, bays and fjords*. Springer Netherlands.
- Nordstrom, K.F., Jackson, N.L., 2012. Physical processes and landforms on beaches in short fetch environments in estuaries, small lakes and reservoirs: A review. *Earth-Science Reviews*, 111(1), 232-247.
- Novak, K., 1992. Rectification of digital imagery. *Photogrammetric engineering and remote sensing*, 58, 339-339.
- OEH, 2018. *Estuaries of NSW*. Office of Environment and Heritage.
- Qiao, G., Mi, H., Wang, W., Tong, X., Li, Z., Li, T., Liu, S., Hong, Y., 2018. 55-year (1960–2015) spatiotemporal shoreline change analysis using historical DISP and Landsat time series data in Shanghai. *International Journal of Applied Earth Observation and Geoinformation*, 68, 238-251.

- Rocchini, D., Metz, M., Frigeri, A., Delucchi, L., Marcantonio, M., Neteler, M., 2012. Robust rectification of aerial photographs in an open source environment. *Computers & Geosciences*, 39, 145-151.
- Roy, P.S., Williams, R.J., Jones, A.R., Yassini, I., Gibbs, P.J., Coates, B., West, R.J., Scanes, P.R., Hudson, J.P., Nichol, S., 2001. Structure and Function of South-east Australian Estuaries. *Estuarine, Coastal and Shelf Science*, 53(3), 351-384.
- Ruggiero, P., Kaminsky, G.M., Gelfenbaum, G., 2003. Linking proxy-based and datum-based shorelines on a high-energy coastline: implications for shoreline change analyses. *Journal of Coastal Research*, 57-82.
- Shand, T., Goodwin, I., Mole, M., Carley, J., Browning, S., Coghlan, I., Harley, M., Preston, W., 2010. NSW coastal inundation hazard study: coastal storms and extreme waves. Water Research Laboratory Technical Report, pp. 1-45.
- Short, A., Trenaman, N., 1992. Wave climate of the Sydney region, an energetic and highly variable ocean wave regime. *Marine and Freshwater Research*, 43(4), 765-791.
- Short, A.D., 1993. *Beaches of the New South Wales Coast; a guide to their nature, characteristics, surf and safety*. Sydney University Press, Sydney.
- Vila-Concejo, A., Austin, T.P., Harris, D.L., Hughes, M.G., Short, A.D., Ranasinghe, R., 2011. Estuarine beach evolution in relation to a flood-tide delta. *Journal of Coastal Research*, 190-194.
- Vila-Concejo, A., Gallop, S.L., Largier, J.L., 2020. Sandy beaches in estuaries and bays. In: D.W.T. Jackson, A.D. Short (Eds.), *Sandy Beach Morphodynamics*. Elsevier, London.
- Vila-Concejo, A., Hughes, M.G., Short, A.D., Ranasinghe, R., 2010. Estuarine shoreline processes in a dynamic low-energy system. *Ocean Dynamics*, 60(2), 285-298.
- Vila-Concejo, A., Short, A., Hughes, M., Ranasinghe, R., 2007. Flood-tide delta morphodynamics and management implications, Port Stephens, Australia. *Journal of Coastal Research*, 50, 705-709.
- Wilson, K.M., Power, H.E., 2018a. Seamless bathymetry and topography dataset for Botany at 10m gridsize. PANGAEA.
- Wilson, K.M., Power, H.E., 2018b. Seamless bathymetry and topography dataset for Hawkesbury River at 50m gridsize. PANGAEA.
- Wilson, K.M., Power, H.E., 2018c. Seamless bathymetry and topography dataset for Sydney Harbour (Port Jackson) at 10m gridsize. PANGAEA.

**Declaration of interests**

The authors declare that they have no known competing financial interests or personal relationships that could have appeared to influence the work reported in this paper.

The authors declare the following financial interests/personal relationships which may be considered as potential competing interests:



**HIGHLIGHTS**

- Decadal beach behaviours are *prograding, quasi-stable, retreating* or *storm relict*
- Some estuarine beaches recover in less than 15 years, while others never recover
- Behaviour dictated by exposure, entrance proximity, rivers and flood-tide delta
- Anthropogenic interventions can benefit or be a detriment to estuarine beaches
- Decadal behaviours will assist coastal management and planning in major cities

Journal Pre-proof